ELSEVIER

Journal of Atmospheric and Solar-Terrestrial Physics 70 (2008) 866–878

Journal of ATMOSPHERIC AND SOLAR-TERRESTRIAL PHYSICS

www.elsevier.com/locate/jastp

Peculiar transient phenomena observed by HF Doppler sounding on infrasound time scales

J. Chum*, J. Laštovička, T. Šindelářová, D. Burešová, F. Hruška

Institute of Atmospheric Physics, Academy of Sciences of the Czech Republic, Bocni II/1401, 14131 Praha 4, Czech Republic

Accepted 4 June 2007
Available online 20 July 2007

Abstract

Compared to investigations of the influence of gravity and planetary waves on the ionosphere, the effects of infrasound (periods from about 0.01 s to several minutes) variations have not been studied very much in the last 20 years. Here we present some recent results on peculiar transient phenomena occurring at infrasound timescales, as observed by HF Doppler sounding in the Czech Republic. After a brief description of the measuring equipment for continuous HF Doppler sounding of the ionosphere, we deal with the observations of short-time transient changes that are observed in the Doppler spectrograms in time intervals of a minute or less, and therefore cannot be observed by ionosondes. First, we present examples of S-shaped traces and examine the diurnal and seasonal variation of their occurrence. We show that S-shape phenomena appear to be concentrated near sunset and sunrise. We also discuss the possible source of these disturbances and their relationship to gravity and infrasound waves. Then we show rare patterns with Doppler shifts corresponding to quasi-linear shape (QLS) phenomena in the time–frequency space. Their slope may be positive or negative. We present some of their properties and discuss the possible origin of such a phenomenon. Several potential sources of QLSs were excluded, such as aircrafts, satellites, bolides, meteors, meteorites, thunderstorms or geomagnetic storms. We speculate that QLSs may correspond to the radio waves in the Z-mode reflected at the upper hybrid resonance frequency.

Keywords: Acoustic-gravity waves; Ionospheric effects on radio waves; Ionospheric dynamics; Ionospheric disturbances; Wave propagation

1. Introduction

An HF Doppler technique is a very sensitive method for detecting transient changes in the ionosphere. Davis and Baker (1966) made great progress in the field of frequency variations of ionospherically propagated HF radio signals. Subsequently, many experimental and theoretical studies have followed (e.g., Georges, 1968; Sutcliffe and Poole, 1989; and references therein). The Doppler measurement is usually a part of radar and/or interferometric measurements, which also makes it possible to measure the angle of wave arrival (e.g., Reinisch et al., 1998).

The Doppler technique measures a frequency shift between the transmitted and received signal after its reflection from the ionosphere. This Doppler shift is proportional to the time rate of change of the signal phase path in the ionosphere. This change of the phase path is mainly proportional to the vertical

*Corresponding author. Tel.: +420 267103301; fax: +420 272762528.
E-mail address: jachu@ufa.cas.cz (J. Chum).

1364-6826/$ - see front matter © 2007 Elsevier Ltd. All rights reserved.
doi:10.1016/j.jastp.2007.06.013

movement of the reflection layer. It can also partially depend on the compression or rarefaction of the electron gas frozen onto the field lines. The Doppler shift then arises from a nonzero divergence of electron movement. The compression or rarefaction of electrons can be caused by the field-aligned component of the pulsating magnetic field (see e.g., Sutcliffe and Poole, 1989, for more detail).

In the ionosphere, collisions between neutral particles and ions and electrons couple the dynamics of neutral and ionized components of the atmosphere. The "strength" of this coupling decreases with increasing height; different processes are significant in different height ranges as well. The nature of the coupling depends mainly on the ratio of the neutral-charged particle collision frequency ν to the gyrofrequency ω_c, for both electrons (ω_{ce}) and ions (ω_{ci}), and the direction of neutral wind with respect to magnetic field. A detailed description of the coupling between the neutral and ionized gases is available in e.g., Rishbeth (1997), Heelis (2004) and Laštovička (2006).

Because of this coupling, the HF Doppler technique makes it possible to study the atmospheric gravity waves (AGWs), the pioneering study of which was made by Hines (1960). The HF Doppler technique is also an important observational tool used for studying the effects of infrasonic waves on the ionosphere. These effects have been reviewed by Blanc (1985), Pokhotelov et al. (1995) and Krasnov et al. (2006). There are many mechanisms and sources of infrasound excitation in the atmosphere such as various strong meteorological phenomena (Hedlin et al., 2002), bolides, meteors, solar eclipses, auroral activity, earthquakes, nuclear and strong chemical explosions, rocket and shuttle launches, aircrafts, etc. Some of them contribute to ionospheric variability, as excited atmospheric waves propagate to ionospheric heights and modulate the atmospheric medium including its ionized part.

The HF Doppler sounding of the ionosphere at a frequency of 3.5945 MHz has been in operation at the Institute of Atmospheric Physics (IAP), Prague since January 2004. A relatively low transmitted power (~1 W) and experimental setup makes it possible to operate the system in the common volume with the digisonde DPS-4 located at Průhonice. Thus, we have the continuous Doppler spectrograms in association with ionograms observed once every 15 min. Burešová et al. (2006) used these common volume measurements to develop a method of improving ionogram evaluation and interpretation. A short description of the continuous Doppler sounding system is given in Section 2.

Sections 3 and 4 deal with two types of phenomena: peculiar Doppler shift pattern, S-shapes and quasi-linear shape (QLS) patterns, which cannot be observed by digisondes. Brief conclusions close the paper.

2. HF Doppler system of the IAP and primary data processing

The continuous HF Doppler sounder including special software has been developed at the Institute of Atmospheric Physics (IAP), Prague, Czech Republic. The transmitted frequency 3.5945 MHz is derived from the 10 MHz oven-controlled crystal oscillator (OCXO) by means of direct digital synthesis (DDS). The short time stability of the oscillator is 2×10^{-10}. An OCXO of the same stability and spectral characteristics is also used at the receiving site. The desired frequency is again tuned by means of DDS, but it is shifted 80 Hz away from the transmitted frequency in order to get the signal-to-noise ratio as high as possible. After conversion to lower frequencies, the received signal is digitized by the precise Sigma Delta analogue to digital converter. The sampling frequency is 610.35 Hz. Finally, the data are transmitted via a network to a PC station, where they are stored. The precise time synchronization is ensured by GPS.

The transmitter was placed at the Průhonice observatory (49°59′N, 14°33′E), which is located about 7 km from the receiver, in Prague at the main building of the IAP (50°02′N, 14°28′E). A great advantage of this topological arrangement is the common volume measurement with a digisonde DPS-4 located at Průhonice. The drawback of this arrangement is the strong ground wave that makes the detection of small Doppler shifts (~less than 0.04 Hz) impossible. When necessary, we remove the ground wave in the frequency domain. Of course the reflected wave is removed in that case as well, when its Doppler shift is near zero. On the other hand, the ground wave provides us with a direct verification of the stability of the oscillators and a zero drift line. At the beginning of April 2005, another transmitter was installed at the Panská Ves observatory (50°32′N, 14°34′E) of the IAP located about 60 km north of the IAP in Prague. Thus, the ionospheric reflections points (regions) are about 30 km apart.

The frequency of transmitters was shifted by 4 Hz, so that only one receiver could be used for the reception of the signals from both transmitters—a similar arrangement as that used by Jones et al. (2004).

Since we are using a frequency lying in the amateur band, we are obliged to transmit a call sign each minute. The duration of the call sign is ~5 s. During this time period, the data acquisition is stopped. It means that the maximum uninterrupted time interval that can be processed by the FFT algorithm is ~55 s; thus the best obtainable frequency resolution is $\sim 1/55 = 0.018$ Hz. The interval of ~55 s proved to be fully sufficient because the received signal is often much broader because of a simultaneous reception of multiple rays reflected from different regions of the ionosphere.

The data are visualized by means of spectrograms. We usually apply a time resolution of 1 min and display 8 h of the record to get the basic overview of the wave activity and the Doppler shift behaviour. We call this kind of spectrogram an "overview spectrogram". In order to be able to study faster changes, for selected cases we make the successive spectral analysis by shifting a Gaussian window of the width ~1 s to ~10 s by a time step much less than the width of the window in the time domain within each acquisition period (~55 s). This technique makes the analysis of higher frequency waves possible, down to periods ~10 s. Of course the frequency resolution is reduced in these cases.

3. S-shapes

Our Doppler shift measurements display two types of transient phenomena on infrasound timescales of a few seconds to a few minutes: S-shapes and linear or QLS patterns. These transient changes of Doppler shift are difficult to recognize in the overview spectrograms displayed on the timescale of 8 h; therefore, we use detailed spectrograms for their analysis. First we deal with S-shapes, various examples of which are shown in Fig. 1.

We have observed many of such S-shaped traces. Their shapes and magnitudes vary, but the basic S-shape is always present. Their typical duration is ~1 min, but some of them cover a time span of several minutes or only tens of seconds. Fig. 1

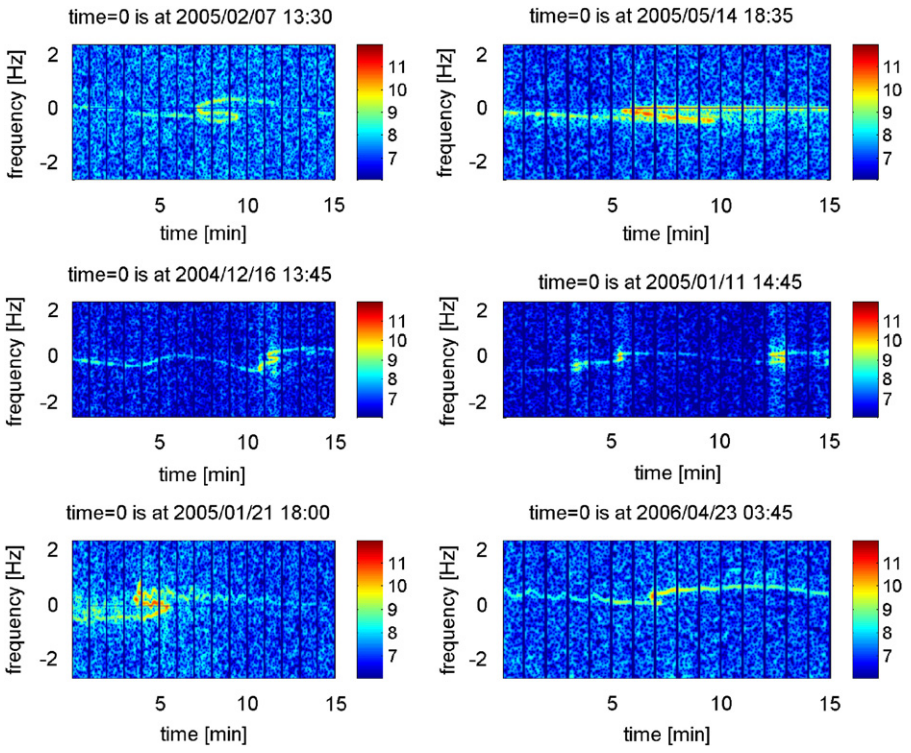

Fig. 1. The variety of S-shapes, some of them with superposed short-timescale waves in the detailed Doppler shift spectrograms of 15 min length. Time in UT (LT-1 h).

presents selected examples of these S-shapes. The upper two spectrograms demonstrate well-developed S-shape phenomena. The two spectrograms in the middle show S-shapes that are either superposed or follow closely one after the other. On the spectrograms at the bottom can be seen S-shapes superposed with infrasonic waves or magneto-hydrodynamic waves (plasma waves propagating at frequencies lower than the cyclotron frequencies of ions). We note that in all these cases the reflection height estimated from the digisonde in Pruhonice is ~300 km.

The S-shaped traces are believed to be formed by reflection from a disturbance of the reflecting level, a level of constant electron density, which has a concave shape and moves horizontally or nearly horizontally (Davis and Baker, 1966; Georges, 1968). As this concave-shaped disturbance moves and enters sounding region, the radio wave reflection becomes forward oblique, which results in longer phase path, negative Doppler shift and forwarded time (first part of S). When the radio wave reflects vertically from the centre of the disturbance, there is no Doppler shift. Then the reflection turns to oblique backward and path length is reduced. Finally, the reflection comes back to vertical, forming the second part of S (see Fig. 5 in Davis and Baker, 1966).

Although S-shapes occur on the infrasonic timescales in the Doppler shift spectrograms, some observations suggest that they are just parts (peaks) of "non-sinusoidal" AGWs. Indeed, Georges (1968) showed that contours of electron density have non-sinusoidal character in the presence of distinct atmospheric waves. The close relationship between AGW and S-shape occurrence is obvious from Fig. 2, which shows a 90-min Doppler shift spectrogram. A distinct, relatively large-scale S-shape is observed as a part of AGW of period ~20 min at time ~45 min from the beginning of the spectrogram. Another interesting example of the S-shape observation was recorded on 15 March 2006. One hour-long spectrogram is presented in Fig. 3. The bottom trace corresponds to the transmitter located at Panska Ves ~60 km northward from the receiver, whereas the upper trace shows the evolution of Doppler shift of the signal from the transmitter located at Pruhonice in the vicinity (~7 km) of the receiver. Both traces show an obvious correspondence; thus the same wave was observed on both signals. (Note that we also receive a strong ground wave from the Pruhonice transmitter, which is seen as a straight line of zero Doppler shift in the spectrogram shifted by 3.7 Hz from zero line of the Panska Ves path.) Since the reflection points are separated in space, sometimes

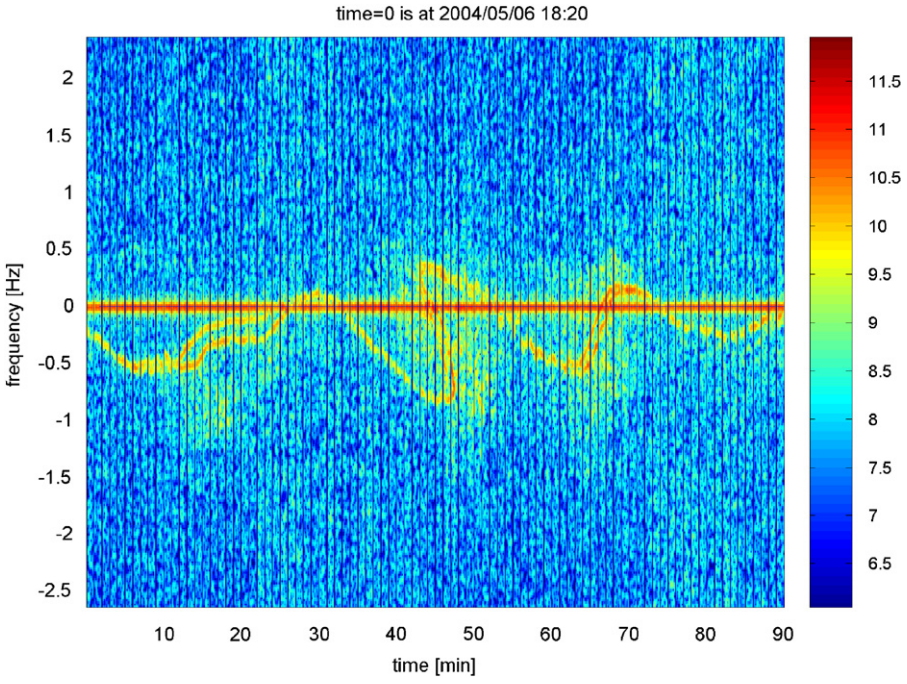

Fig. 2. Example of S-shaped trace as a part of AGW. Time in UT (LT-1 h).

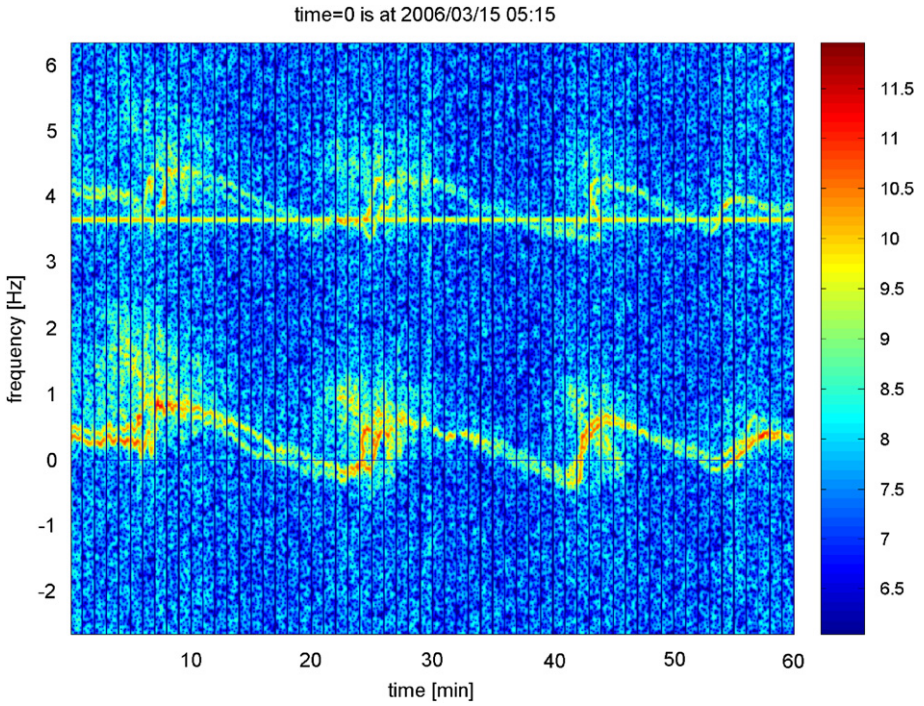

Fig. 3. Example of the observation of AGWs with S-shaped trace observed in two different regions separated horizontally by ~35 km. Time in UT (LT-1 h).

the reflected signals are not exactly identical. Such a situation represents the third peak (~45 min on the time axis), when we observed a S-shape on one signal and a non-sinusoidal wave on the other. There is also a time delay (phase shift) between both signals. Looking at different peaks or zero crossings, we can see that this time delay changes with time during the observation. Since we have only two-point measurement, we cannot determine velocity and azimuth of the propagation. With a multipoint measurement we would be able to determine vector of motion. A systematic study of propagation directions of such waves and disturbances, and their dependence on season, daytime, geomagnetic and other conditions will be a subject of future study after the installment of multipoint measurements.

Despite the fact that we have shown that there is a close relationship between some AGWs and S-shape occurrence, we cannot exclude the fact that in some cases the S-shape observations are caused by small-scale ''solitary'' disturbances that propagate in infrasonic or magneto-hydrodynamic wave mode. For example, the relationship between AGWs and S-shapes presented in the middle spectrograms in Fig. 1 is not clear. It is possible that in this case we observe either superposition (interference) of AGWs or disturbances propagating in other wave modes. We cannot exclude the fact that these disturbances are formed by infrasound excited at the surface by (quasi)point sources, the energy of which is focused by the troposphere and middle atmosphere upwards into a narrow cone (e.g., Blanc, 1985; Krasnov et al., 2006), which then broadens again in the ionosphere. Nevertheless, a source of the S-shapes at higher altitudes like the solar terminator or other mechanisms of their excitation is more probable as suggested by the following statistical study; the terminator can excite infrasonic waves similar to proven excitation of gravity waves (e.g., Boška et al., 2003).

As far as we know, the diurnal and seasonal distribution of S-shape occurrences has not yet been studied systematically. A first step of such a study is presented in Fig. 4, which shows diurnal and seasonal distribution of all sufficiently pronounced S-shape events, each observed on both radio paths during 1-year-long interval. The statistics is based on manual data retrieval from spectrograms. A well-pronounced tendency of S-shape events to occur near sunrise and sunset is evident. Around midday the recorded Doppler shift is small and the

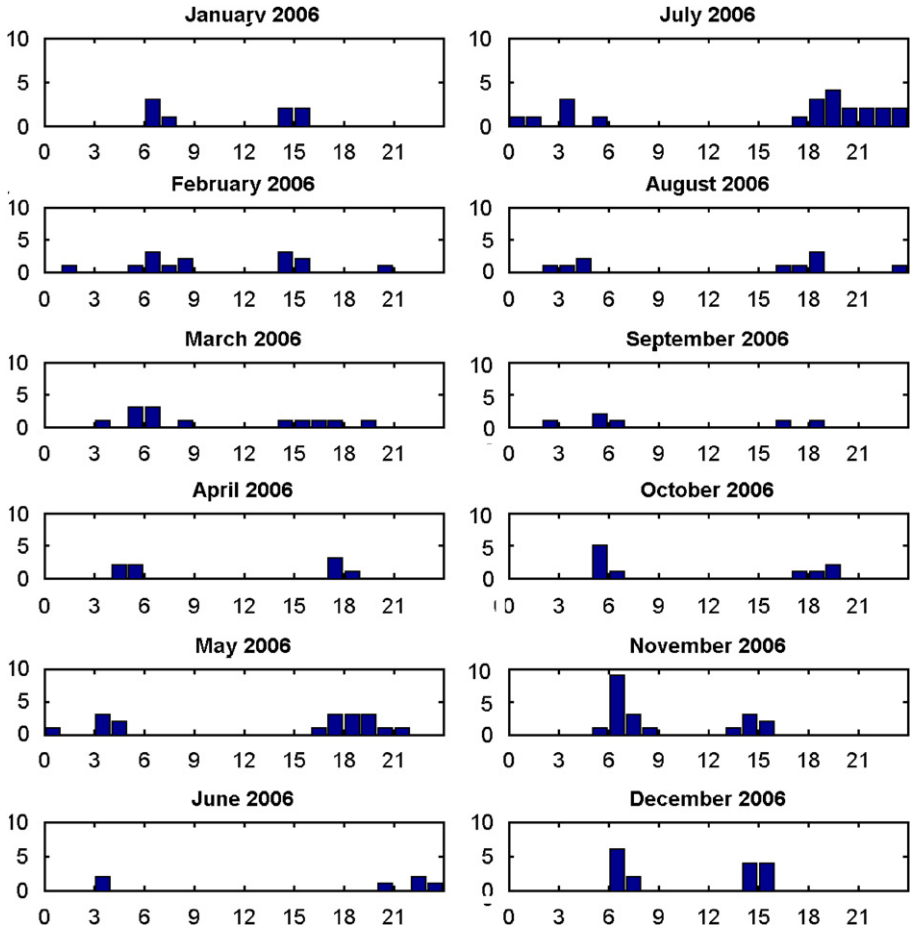

Fig. 4. Diurnal and seasonal distribution of all sufficiently pronounced S-shape disturbances, each detected on both paths, observed in the period April 2005–March 2006.

signal is weak, sometimes even below the noise threshold, which may artificially reduce the number of observed daytime S-shapes. Fig. 4 also shows that no well-pronounced seasonal variation of the S-shape phenomenon is observed in terms of the total number of S-shape events per month, even though 1 year is too short a period to make reliable conclusions about seasonal variation. On the other hand, there is a pronounced seasonal variation of diurnal distribution of the S-shape events, which is closely related to the sunset times as they change with seasons. The solar terminator during sunset and particularly sunrise is known to excite gravity waves (e.g., Somsikov, 1995; Boška et al., 2003) in the ionosphere and the diurnal variation of gravity wave activity peaks near sunrise and sunset (e.g., Boška et al., 2003). The solar terminator excites various inhomogeneities and waves; therefore we may also expect excitation of inhomogeneities or waves in the infrasound time-scale range. On the other hand, a few S-shapes occur well before or after sunrise and sunset (Fig. 4) and, therefore, cannot be related to the solar terminator. Thus, also other mechanisms and sources probably exist, which are responsible for the formation of the S-shapes in the Doppler shift spectrograms.

4. Quasi-linear shape (QLS) phenomenon

Other peculiar transient phenomena are patterns of linear or QLSs) in the Doppler shift spectrograms. These patterns usually have much greater Doppler shifts than normal signals, and their origin is unclear. They usually last a few tens of seconds, and their frequency span can be up to several tens of Hertz. In some cases, the sign of the Doppler shift changes during a single observation as if an object

was first approaching (moving away), then started to move away (approach), all the time having a nearly constant change of Doppler shift with time, i.e. nearly constant acceleration or deceleration. The spectral power of the Doppler shift of these QLSs is similar to the spectral power of the normal signal reflected from the ionosphere. As far as we know, observations of QLSs have not yet been reported. Various examples of QLSs are present in Fig. 5. Note that for the sounding frequency 3.5945 MHz, the Doppler shift of 1 Hz corresponds to the vertical velocity of 41.7 m/s.

In the same way as we did for S-shapes, we have performed a simple statistical study of QLS occurrence in dependence on daytime and season. We have included only distinct QLSs with the Doppler frequency span greater than ~3 Hz in this study. Fig. 6 shows the diurnal distribution of observed QLS from 1 September 2004 to 31 August 2006. It is obvious that most of the distinct QLSs are observed near sunset or in early night-time hours. Some of them also occur in the late night or in the morning. Well into the daytime, the radio wave absorption in the D region is relatively high at the sounding frequency and the E-region blocking might be an issue. However, we analyse observations made under low solar activity conditions and, therefore, over most of the time we still have record and can identify QLSs, if they occur. The situation with the daytime signal will be worse after 3–5 years under the solar cycle maximum conditions. Thus, the absorption and E-region screening can somewhat reduce the number of identified QLSs, but in no way can be responsible for their absence during daytime. The drop-off in their occurrence frequency after about 21 UT (22 LT) could be related to the night-time decrease of foF2, particularly because we analyse measurements under low solar activity conditions, but inspection of records shows that the reflection of the sounding signal is rarely missing. This effect will be even smaller under high solar activity conditions. Thus, this effect can somewhat but not significantly contribute to the observed diurnal distribution of QLSs. The QLS phenomenon is predominantly related to the near-sunset and post-sunset conditions; it is not an artefact of the measuring technique.

Fig. 7 presents the distribution of observed QLSs, with frequency span greater than 3 Hz, during the 2 years of observation. QLSs tend to appear in

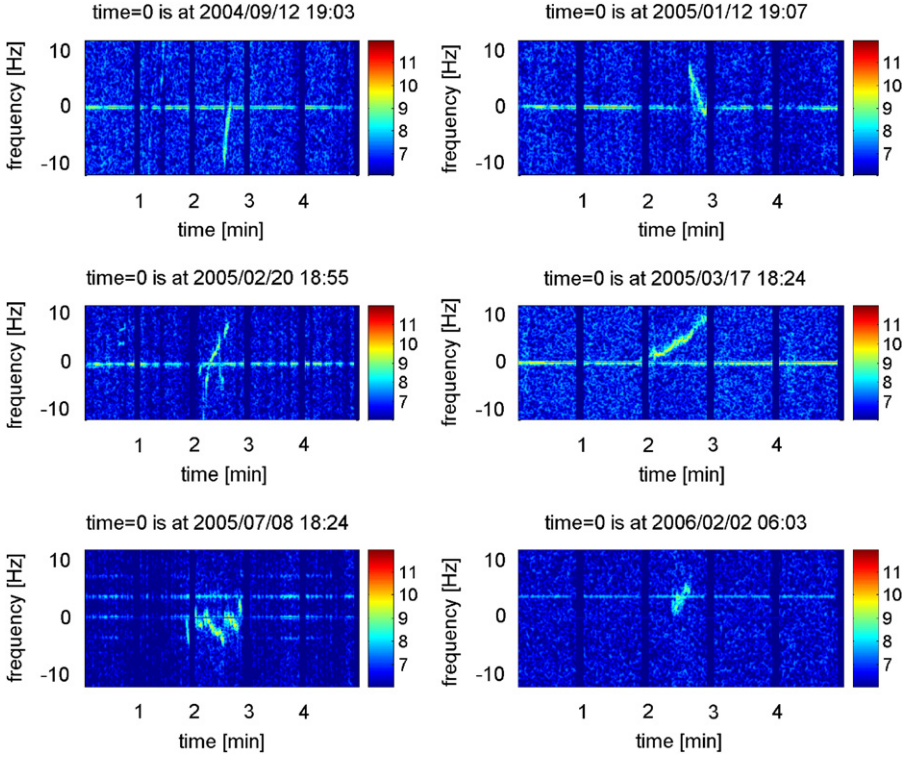

Fig. 5. Examples of various QLSs in detailed Doppler shift spectrograms. Time in UT (LT-1 h).

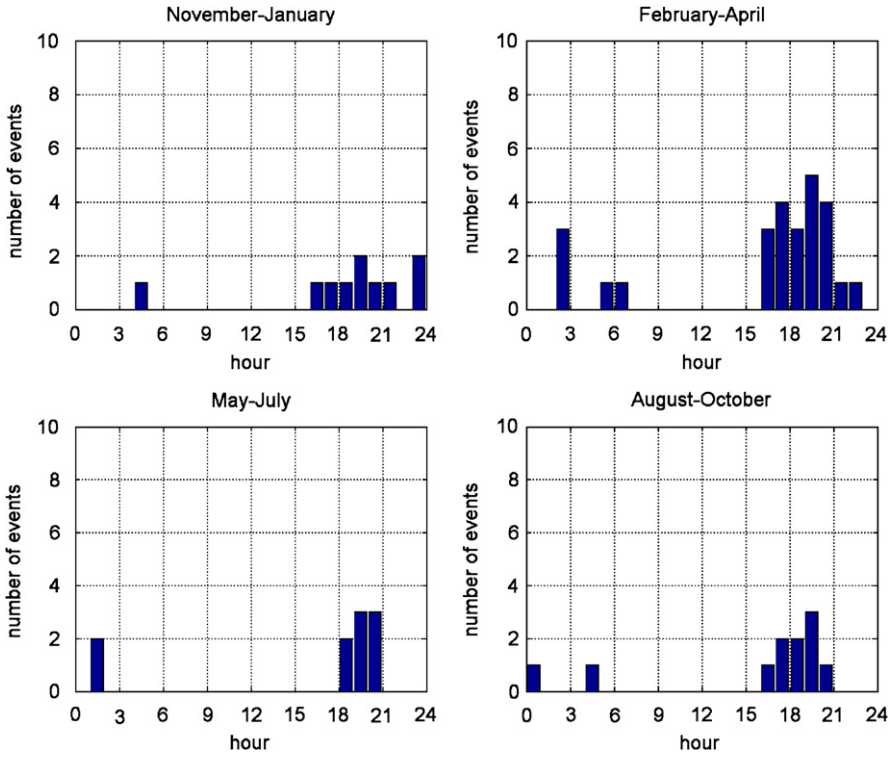

Fig. 6. Diurnal/seasonal distribution of QLSs observed from 1.9.2004 to 31.8.2006. Time in UT (LT-1 h).

clusters but they do not display an evident seasonal variation. We should mention that distinct QLSs are a very rare phenomenon; therefore the presented results are based on a relatively small amount of data and must be considered with caution. We should also mention that we searched for QLSs in the spectrograms visually.

The number of QLS events is relatively small, 57. Therefore it is necessary to test if the diurnal and seasonal distributions are random or not. Applying the test of randomness and other statistical analyses from the StatGraphics software package, we find that the diurnal distribution is not random at a level higher than 95%. On the other hand, the seasonal distribution of QLSs is random, which is consistent with the absence of a pronounced seasonal variation.

QLSs included in our statistical survey have different slopes and lengths in frequency–time space. Fig. 8 shows dynamic characteristics of the observed QLSs. It presents the occurrence histograms of their frequency span, time span and slopes in the frequency–time plane. QLS patterns have the most often occurring frequency span of 5–10 Hz, median span 10–15 Hz and mean span 15–20 Hz; they last typically about 20 s, and have a typical slope of 0.4–0.5 Hz/s, which corresponds to an acceleration of about 20 m/s^2. A positive slope is more probable than the negative slope.

Regarding the geomagnetic and ionospheric conditions, most distinct QLSs have been observed during geomagnetically quiet or moderately disturbed days (K_p from 0 to 4+), but not during high geomagnetic activity, which means that geomagnetic storms are not likely responsible for QLSs. In a few cases, ionograms detect the presence of a sporadic E-layer during the observation of QLS, but in most of the recorded events a sporadic E-layer was not present.

The occurrence of QLS in the Doppler shift spectrogram usually does not influence the intensity of normal reflected signal (sometimes a partial attenuation is observed during the observation of QLS). A question arises: what causes the observation of QLS?

First, we exclude several possible sources of the observed echoes (QLSs). Taking into account the vacuum wavelength of the sounding radio signal of 83.4 m and the requirement of minimum size of reflecting body to be $\lambda/2$, i.e. 41.7 m, we can exclude (military) supersonic aircrafts as a potential source

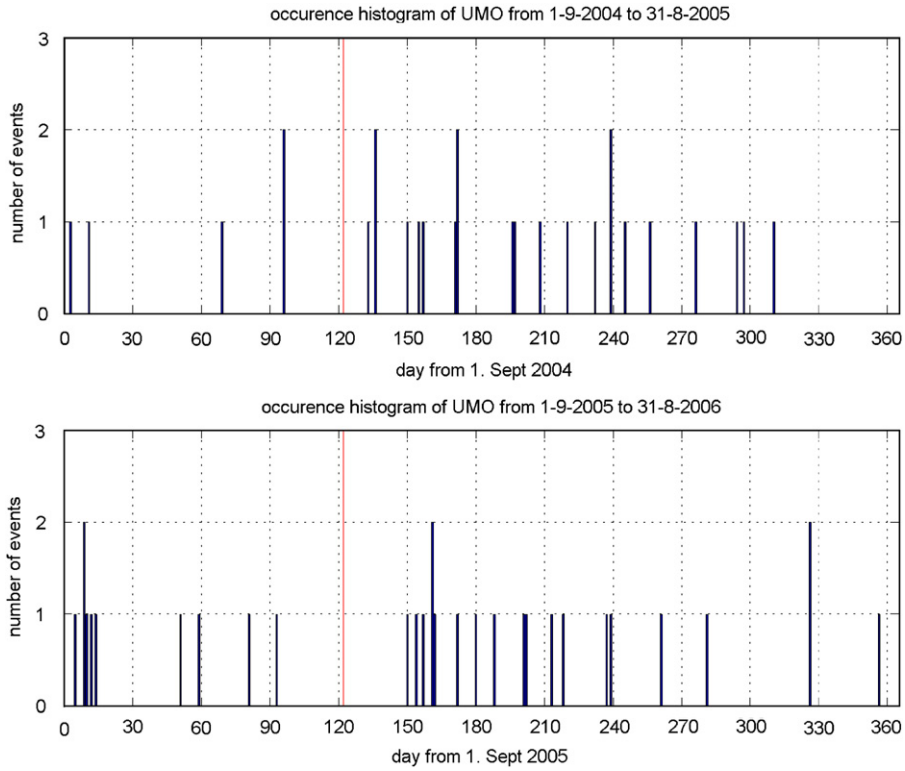

Fig. 7. Distribution of QLSs within the period from 1.9.2004 to 31.8.2006. Red vertical lines indicate the beginnings of the new calendar year.

of QLSs, as such aircrafts flying over Czech territory are too small. However, big commercial subsonic aircrafts fulfil the condition of sufficient size. Aircraft traces, observed with Doppler systems at substantially higher radio frequencies, show that these traces on recordings last significantly longer than QLSs; thus we may exclude commercial subsonic aircrafts as a source of the observed QLSs. Examples may be found at http://www.qsl.net/g3cwi/doppler.htm

Moreover, the velocity of subsonic aircrafts cannot explain the high values of Doppler shift which are consistent with supersonic velocities.

We made a comparison between observed bolides in the Czech Republic, particularly those distant no more than 50–100 km from the reflection points of HF Doppler radio paths, and QLSs. This comparison shows no coincidence between the observed bolides and QLSs.

It is also difficult to imagine a motion of a meteor in the case that the slope of QLS is positive (rising in frequency) and the trace of QLS crosses the zero frequency in the Doppler shift spectrogram. That would mean that such a meteor should move away first and then approach.

We also discarded the possibility that we observe echoes from ionized traces produced by meteors and meteorites. Such traces are produced mostly in the mesopause region and the mesosphere, where they move with neutral wind (they are even used by meteor radars to measure neutral wind). The wind is very predominantly horizontal with speeds of tens of m/s, which cannot produce the observed Doppler shifts.

Similarly, the typical duration of the observation of QLSs—tens of seconds—and the non-coincidence with thunderstorm occurrence exclude the sprite-related sounding radio wave reflections and other possible thunderstorm-related effects.

Another possibility is reflection from satellites. Most of them are too small, but the size of the International Space Station (ISS) is comparable with the wavelength of the sounding radio wave; the inclination of ISS is 51.6°. We analysed ionograms in the vicinity of QLS events. Manually checked ionograms provide for QLS events the range of the height of the maximum of the F2 layer (hmF2) 210–350 km with median and mean values between 280 and 290 km; QLS reflection heights are

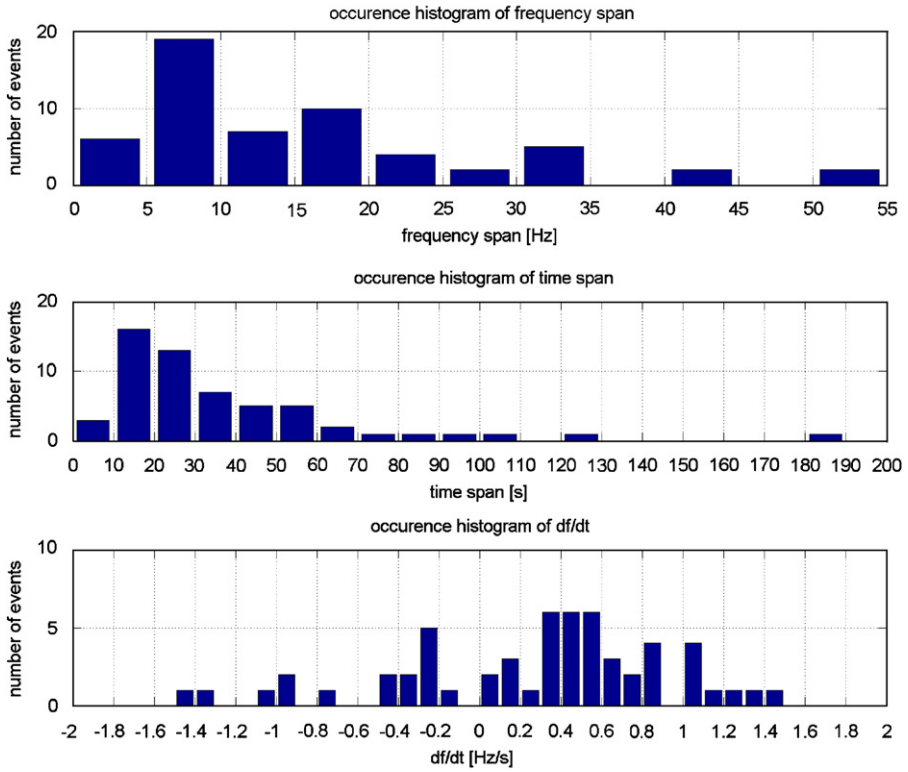

Fig. 8. Dynamic characteristics of QLSs.

somewhat lower than hmF2. The altitude of the ISS is 321–351 km, i.e. most QLS reflections were well below the ISS height, but a few of them might be from ISS heights. Note also that the transmitted power is only ~1 W. Concerning this rather low transmitted power, the altitude of ISS and its size, which is comparable to the wavelength of the transmitted wave, it is improbable that the signal reflected from ISS would have a similar strength as the signal reflected from the ionosphere. Moreover, we found no coincidence between QLS occurrence and passes of the ISS over the Czech territory or its vicinity.

Of course, we cannot rule out that we observe some kind of natural emission. We also cannot exclude the observation of artificial signals. Nevertheless, due to the systematic appearance of QLSs in the late evening or early night-time and because of their narrow width and spectral power comparable with normal signal, we think that they are natural phenomena. Perhaps, they could be associated with some dynamic transient natural enhancements of plasma density in the lower part of the ionosphere.

As much more probable, we consider the hypothesis based on the assumption that the QLS traces in spectrograms are formed by the transmitted radio wave rays, which were converted to Z-mode before their reflection in the ionosphere. To elucidate this idea, we first summarize the properties of the dispersion relation for electromagnetic waves in cold magnetized collisionless plasma. This dispersion relation is a quadratic equation for the square of the refractive index n. Thus, maximally two different modes can propagate at specific frequency in cold plasma (Stix, 1992). Fig. 9 shows the refractive index squared for waves propagating with different angle θ of wave vector k to magnetic field direction in dependence on frequency normalized to the electron cyclotron frequency $\omega_c = 2\pi f_c$ in the frequency range of interest. Since in the ionosphere, at latitudes ~50°, f_c equals ~1.2 MHz, which is less than the plasma frequency f_p in the altitude where the wave of the transmitted frequency 3.59 MHz undergoes the reflection, we investigate the case when $\omega_p > \omega_c$.

From Fig. 9, it is obvious that the only modes which can escape from plasma and which are

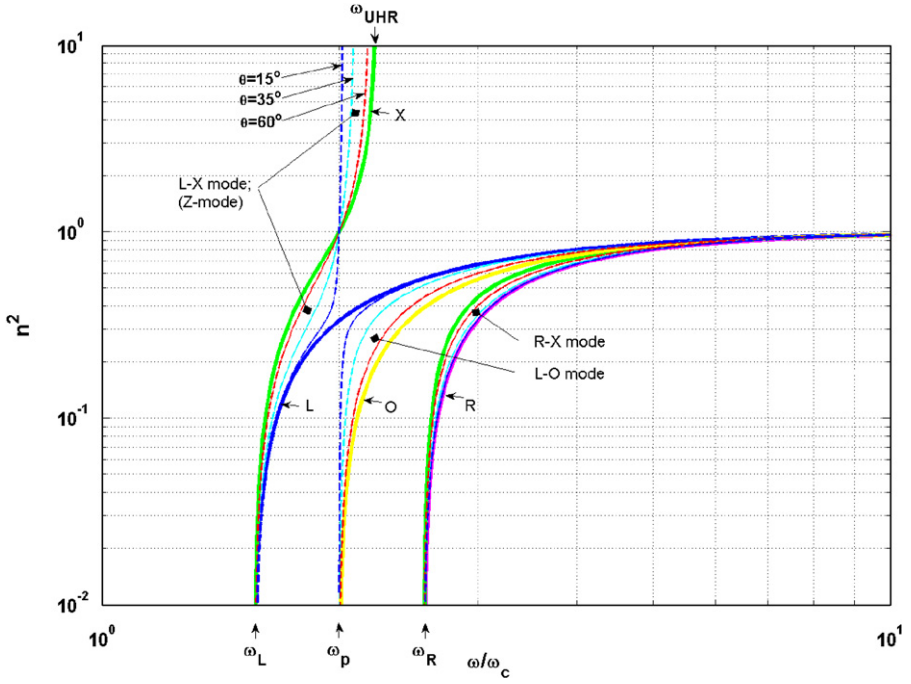

Fig. 9. Dispersion diagram—square of refractive index n in dependence on wave frequency ω normalized to electron cyclotron frequency ω_c for electromagnetic waves in cold magnetized plasma in the frequency region of interest. Different colours and line widths distinguish different angles θ between wave vector $\boldsymbol{k}$ and ambient magnetic field. A common notation is used; R (L) stands for a right-handed (left-handed) circularly polarized wave with $\theta = 0$, O is used for a linearly polarized ordinary wave with $\theta = 90^\circ$ and wave electric field oscillating along the magnetic field lines, and X represents a linearly polarized extraordinary wave with $\theta = 90^\circ$ and wave electric field oscillating perpendicularly to the field lines. Next, ω_L (ω_R) is a cut-off frequency for L-X (R-X) mode, ω_p is a plasma frequency, which is a cut-off for L-O mode, and ω_{UHR} is the upper hybrid resonance frequency.

directly accessible from free space are R-X mode propagating above the ω_R cut-off frequency, and L-O mode propagating above the plasma frequency ω_p. Both these modes have refractive index $n \leqslant 1$. The left-handed circularly polarized wave propagates exactly along a magnetic field line with $\theta = 0$; in other words the pure L-mode represents a singularity in the dispersion relation and has a cut-off frequency ω_L. This cut-off frequency is however important for the L-X mode, which is also called Z-mode. The Z-mode can only propagate in the frequency range $\omega_L < \omega < \omega_{UHR}$, where ω_{UHR} is the upper hybrid resonance (UHR) frequency. The Z-mode has $n < 1$ in the frequency range $\omega_L < \omega < \omega_p$ (also called super-luminous Z-mode since the phase velocity is greater than the speed of light c in free space), and $n > 1$ in the frequency range $\omega_p < \omega < \omega_{UHR}$ (also called sub-luminous Z-mode since the phase velocity is less than c). Between the above-discussed frequencies the following relation holds:

$$\omega_L < \omega_p < \omega_{UHR} < \omega_R. \quad (1)$$

When a radio wave transmitted from the ground reaches the lower parts of the ionosphere, it starts propagating in L-O mode or R-X mode or in both depending on the initial angle of wave vector to magnetic field and initial wave polarization. As the wave propagates upwards, the frequencies in Eqn. (1) increase and become comparable with the wave frequency. If the wave frequency is low enough, the wave reaches the height where its frequency is equal to the cut-off frequency and reflects downward, first the R-X mode ($\omega \sim \omega_R$) and then the L-O mode ($\omega \sim \omega_p$). However, some portion of waves propagating in L-O mode with wave vector sufficiently close to magnetic field line direction may convert to L-X mode. If plasma density continues increasing along the wave trajectory, the L-X mode wave will reflect at the ω_L cut-off and will experience a Doppler shift as do R-X and L-O waves. A different situation arises, if for some reason the plasma density starts decreasing before the L-X wave reaches the ω_L cut-off. Such a wave will finally propagate in the sub-luminous Z-mode

($n>1$) until it approaches a region where $\omega = \omega_{UHR}$. Since it cannot propagate into the region where $\omega > \omega_{UHR}$, it will strongly refract—in other words reflect backwards. Such a reflection, however, takes place for a wave with $n \gg 1$. Since $n = kc/\omega$ and the observed Doppler shift $\Delta\omega$ is given by

$$\Delta\omega \sim -2 \cdot k \cdot v, \quad (2)$$

where v is the velocity of background plasma in the region of reflection, the wave reflecting in Z-mode close to $\omega = \omega_{UHR}$ will experience a distinct Doppler shift, greater than waves reflecting due to cut-off frequencies. The reflected wave can again convert into the L-O mode during its backward propagation and reach the ground.

The "necessary" decrease of plasma density may be caused by various reasons like the presence of a valley between the ionospheric layers, large-scale inhomogeneities, vertical waviness, or by propagating above the density maximum of the ionosphere.

If the conditions for waves to convert into Z-mode and to reflect at $\omega \sim \omega_{UHR}$ lasted several tens of seconds, and if we take into account that the typical periods of gravity waves and other motion of a background plasma are of the order of ~20 min, then the Z-mode reflected waves would have been influenced just by a very short interval of a gravity wave, and it is expectable that such a part will have a linear or QLS in the Doppler shift spectrogram, exactly as QLSs have.

We think that the proposed hypothesis may explain the basic features of QLSs; nevertheless more theoretical and experimental investigations are needed to verify it. An important experimental test can be the measurement of polarization of QLS signals. If the above proposed hypothesis is correct, then the QLSs should be received with L-O polarization on the ground. Unfortunately, our current instrumentation does not allow such measurements.

5. Conclusions

We have presented the first results of our Doppler sounding system observations of two transient peculiar phenomena, occurring on the infrasound timescales: S-shapes and so-called quasi-linear shapes (QLSs).

The S-shape disturbances are produced, likely, by reflection from the concave-shaped irregularities of reflecting level. They tend to occur very preferentially near sunrise and sunset, which suggests that at least some of them may be caused by solar terminator effects. The systematic study of their propagation is worthy of future investigation. The occurrence of S-shapes does not seem to have a well-pronounced seasonal variation. We demonstrated and discussed the relationship of S-shape observations to infrasound and atmospheric gravity waves.

We presented the observation of QLS phenomena sometimes found in the Doppler shift spectrograms. They mostly occur in the early night or in the late evening. They have QLS in the frequency–time space with both negative and positive slopes, and both signs of Doppler shift. A typical QLS has a frequency span around 10 Hz, a duration of about 20 s and a slope about 0.4–0.5 Hz/s.

We discussed the possible origin of QLSs. We excluded/discarded several potential sources of QLSs such as aircrafts, satellites, bolides, meteors, meteorites, thunderstorms or geomagnetic storms. We speculate that QLSs are formed by radio waves that propagate in the Z-mode in the ionosphere and reflect in the region of negative density gradient along the up-going part of their ray trajectory at $\omega \sim \omega_{UHR}$ (upper hybrid resonance frequency).

Future investigations of peculiar transient phenomena will be mainly based on the multipoint HF Doppler shift measurements supported by ground-based measurements of infrasound, both to be installed in the next 1–2 years. We consider the possibility of measurements of signal (wave) polarization.

Acknowledgements

This work was supported by the Grant Agency of the Czech Republic through Grant nos. 205/04/2110 and 205/07/1367.

References

Blanc, E., 1985. Observations in the upper atmosphere of infrasonic waves from natural or artificial sources: a summary. Annales Geophysicae 3, 673–688.

Boška, J., Šauli, P., Altadill, D., Solé, G., Alberca, L.F., 2003. Diurnal variation of the gravity wave activity at midlatitudes of the ionospheric F region. Studia Geophysica et Geodaetica 47, 578–586.

Burešová, D., Krasnov, V., Drobzheva, Ya., Laštovička, J., Chum, J., Hruška, F., 2007. Assessing the quality of ionogram interpretation using the HF Doppler technique. Annales Geophysicae 25, 895–904.

Davis, K., Baker, D.M., 1966. On frequency variations of ionospherically propagated HF radio signals. Radio Science 1, 545–556.

Georges, T.M., 1968. HF Doppler studies of travelling ionospheric disturbances. Journal of Atmospheric and Terrestrial Physics 30, 735–746.

Hedlin, M.A.H., Garces, M., Bass, H., Hayward, C., Herrin, G., Olsen, J., Wilson, C., 2002. Listening to the secret sounds of Earth's atmosphere. EOS Transactions of AGU 83 (48), 557–565.

Heelis, R.A., 2004. Electrodynamics in low and middle latitude ionosphere: a tutorial. Journal of Atmospheric and Solar-Terrestrial Physics 66, 825–838.

Hines, C.O., 1960. Internal atmospheric gravity waves at ionospheric heights. Canadian Journal of Physics 38, 1441–1481.

Jones, T.B., Wright, D.M., Milner, J., Yeoman, T.K., Reid, T., Chapman, P.J., Senior, A., 2004. The detection of atmospheric waves produced by the total solar eclipse of 11 August 1999. Journal of Atmospheric and Solar-Terrestrial Physics 66, 363–374.

Krasnov, V.M., Drobzheva, Y.a.V., Laštovička, J., 2006. Recent advances and difficulties of infrasonic wave investigation in the ionosphere. Surveys in Geophysics 27, 169–209.

Laštovička, J., 2006. Forcing of the ionosphere by waves from below. Journal of Atmospheric and Solar-Terrestrial Physics 68, 479–497.

Pokhotelov, O.A., Parrot, M., Fedorov, E.N., Pilipenko, V.A., Surkov, V.V., Gladychev, V.A., 1995. Response of the ionosphere to natural and man-made acoustic sources. Annales Geophysicae 13, 1197–1210.

Reinisch, B.W., Scali, J.L., Haines, D.M., 1998. Ionospheric drift measurements with ionosondes. Annali di Geofisica 41, 695–702.

Rishbeth, H., 1997. The ionospheric E-layer and F-layer dynamos—a tutorial review. Journal of Atmospheric and Solar-Terrestrial Physics 59, 1873–1880.

Somsikov, V.M., 1995. On the mechanism for the formation of atmospheric irregularities in the solar terminator region. Journal of Atmospheric and Terrestrial Physics 57, 75–83.

Stix, T.H., 1992. Waves in Plasmas. American Institute of Physics, New York.

Sutcliffe, P.R., Poole, A.W.V., 1989. Ionospheric Doppler and electron velocities in the presence of ULF waves. Journal of Geophysical Research 94 (A10), 13505–13514.